International Journal of Information, Control and Computer Sciences
ISSN: 2517-9942
Vol:10, No:7, 2016

Experimenting with Error Performance of Systems Employing Pulse Shaping Filters on a Software-Defined-Radio Platform

Chia-Yu Yao

***Abstract*—**This paper presents experimental results on testing the symbol-error-rate (SER) performance of quadrature amplitude modulation (QAM) systems employing symmetric pulse-shaping square-root (SR) filters designed by minimizing the roughness function and by minimizing the peak-to-average power ratio (PAR). The device used in the experiments is the 'bladeRF' software-defined-radio platform. PAR is a well-known measurement, whereas the roughness function is a concept for measuring the jitter-induced interference. The experimental results show that the system employing minimum-roughness pulse-shaping SR filters outperforms the system employing minimum-PAR pulse-shaping SR filters in the sense of SER performance.

***Keywords*—**Pulse-shaping filters, jitter, inter-symbol interference, symmetric FIR filters, QAM

I. Introduction

SQUARE-ROOT (SR) pulse-shaping filters are widely used in a band-limited communication systems, in which an SR filter $h_t[n]$ is placed at the transmitter and its corresponding matched SR filter $h_r[n]$ is placed at the receiver, as shown in Fig. 1. Conventionally, the SR filters are designed by directly designing the zero-phase Nyquist filter with a nonnegative frequency response, then getting the matched SR transmitter and receiver filters via a spectral factorization of the Nyquist filter polynomial. In this way, the obtained SR filters usually have asymmetric coefficients [1]-[7]. Since a linear-phase FIR filter has symmetric coefficients, the required number of multipliers is around a half of the number of its coefficients. Thus, the complexity of a symmetric FIR filter is lower than that of its asymmetric counterpart. Although [8] shows that matched symmetric SR FIR filter pairs cannot lead to zero inter-symbol interference (ISI), [9] and [10] argue that a suitable tolerable ISI suffices to serve as a design constraint that the final SR filter designs will not affect much of the error rate at a certain operating point of a communication system.

In 2008, [11] proposed a method of controlling the tail size of the symmetric SR filter to reduce the peak-to-average power ratio (PAR). In 2012, we presented a concept called the roughness function that reflects the magnitude of the jitter-induced interference [12]. By minimizing the roughness function, [12] showed in simulations that its symmetric SR filter design can lead to a lower error rate comparing with the other SR filter designs in 256-QAM communication systems in the presence of receiver timing jitter.

In simulations of [12], we assume the clock recovery subsystem is perfect; i.e., the sampling clock is coherent with the received signal. However, in many modern communication systems, the receiver employs high-speed ADC to overly sample the received signals. The sampling rate is not synchronous with the received signals well. Under the circumstances, a perfect clock recovery subsystem is not included at the receiver. To further verify the simulation results, this work employs the 'bladeRF' software- defined-radio (SDR) platform[1] to test SER of systems employing the symmetric SR filters designed by minimizing the PAR [11] and by minimizing the roughness function [12], respectively. In the experiments of this work, the knowledge of analog front-ends, as well as the perfect clock recovery circuits on the bladeRF platforms are not available for us.

This paper is organized in the following manner. Section II shows the experiment setup and describes the procedure of the experiments. Section III shows the experimental results of SER. Finally, some conclusion remarks are summarized in Section IV.

II. The Experiment Setup

In Fig. 1, T denotes the oversampling ratio, $Sm(s)$ and $An(s)$ represent the transfer functions of the analog smoothing filter and the analog anti-aliasing filter, respectively , and $h_t[n]$ and $h_r[n]$ denote the matched SR filters. Since we are interested in the symmetric SR filters in this work, $h_r[n] = h_t[N-1-n] = h_t[n]$, where N denotes the SR filter length. In Example 2 of [12], the oversampling ratio $T = 4$. The obtained $h_{t1}[n]$ by minimizing the PAR [11] and the obtained $h_{t2}[n]$ by minimizing the roughness function for the discrete-time case [12] in Example 2 of [12] are re-summarized in Table I. The stopband attenuation (SBATT), the tolerable ISI, the roughness for the discrete-time case (R_d), and the PAR values corresponding to $h_{t1}[n]$ and $h_{t2}[n]$ are summarized in Table II. The formulas of R_d and PAR are given below for convenience.

$$R_d = \sum_n |h_t[n] - h_t[n-1]|^2 \quad (1)$$

Chia-Yu Yao is with the Department of Electrical Engineering, National Taiwan University of Science and Technology, Taipei, Taiwan 106 (e-mail: chyao@mail.ntust.edu.tw).

This work was supported by the Ministry of Science and Technology of Taiwan, ROC, under Grant MOST 104-2221-E-011-121.

[1] BladeRF is the trademark of Nuand LLC.

$$\mathrm{PAR} = T \max_{0 \le i < T} \frac{\sum_k |h_t[kT+i]|^2}{\sum_k h_t^2[k]} \quad (2)$$

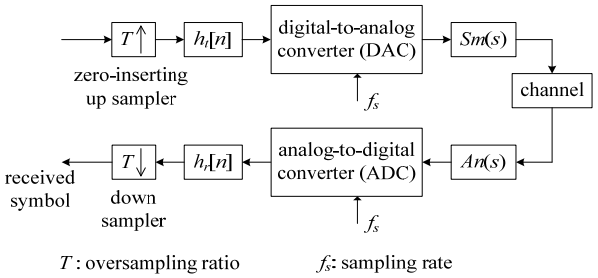

Fig. 1 Block diagram of a band-limited digital communication system

TABLE I
SYMMETRIC SR FILTER COEFFICIENTS OF $H_{T1}[N]$ DESIGNED BY THE METHOD OF [11] AND $H_{T2}[N]$ BY THE METHOD OF [12]

$h_{t1}[n]$: Length = 18, $h_{t1}[n] = h_{t1}[17-n]$, n = 9, 10, . . . , 17	
$h_{t1}[0] = 8.8379630 \times 10^{-3}$	$h_{t1}[5] = 5.2659406 \times 10^{-4}$
$h_{t1}[1] = 7.8090690 \times 10^{-3}$	$h_{t1}[6] = 9.0010548 \times 10^{-2}$
$h_{t1}[2] = -8.1950110 \times 10^{-3}$	$h_{t1}[7] = 1.9864513 \times 10^{-1}$
$h_{t1}[3] = -3.2224399 \times 10^{-2}$	$h_{t1}[8] = 2.7332536 \times 10^{-1}$
$h_{t1}[4] = -3.8555482 \times 10^{-2}$	
$h_{t2}[n]$: Length = 18, $h_{t2}[n] = h_{t2}[17-n]$, n = 9, 10, . . . , 17	
$h_{t2}[0] = 1.2395030 \times 10^{-2}$	$h_{t2}[5] = 4.3568008 \times 10^{-3}$
$h_{t2}[1] = 9.1754965 \times 10^{-3}$	$h_{t2}[6] = 9.7797267 \times 10^{-2}$
$h_{t2}[2] = -8.7540407 \times 10^{-3}$	$h_{t2}[7] = 2.0034947 \times 10^{-1}$
$h_{t2}[3] = -3.9143400 \times 10^{-2}$	$h_{t2}[8] = 2.6750924 \times 10^{-1}$
$h_{t2}[4] = -4.3231239 \times 10^{-2}$	

We employ $h_{t1}[n]$ and $h_{t2}[n]$ in Table I as SR filters in two experiments, respectively. The over-sampling ratio T is set to 4. The SERs measured in two experiments are compared that we can determine whether the SR filter designed by minimizing the roughness function is better or not.

TABLE II
SUMMARY OF THE VALUES OF SBATT, ISI, R_D, AND PAR CORRESPOND TO $H_{T1}[N]$ AND $H_{T2}[N]$ (NO ANALOG PARTS ARE CONSIDERED.)

System	SBATT	ISI	R_d	PAR
$h_{t1}[n]$	24.02 dB	−54.85 dB	0.0557	2.39 dB
$h_{t2}[n]$	25.16 dB	−54.80 dB	0.0549	2.82 dB

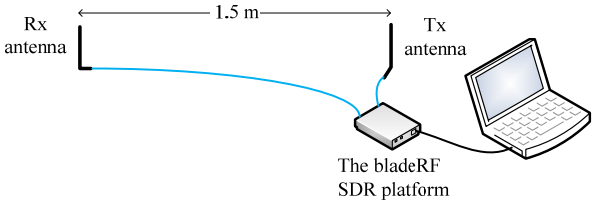

Fig. 2 Experimental setup

In addition to $T = 4$ only, the bladeRF platform does not have a perfect clock recovery circuit, so the sampling clock in the bladeRF platform is not well synchronous with the received signal. Therefore, the experiments cannot hold for high QAM, as we have done in [12]. Hence, we only employ 16 QAM in the experiments.

A. Setup and Procedure

We employ one bladeRF platform and one computer in the experiments. The experimental setup is shown in Fig. 2 and the picture of the experiment is shown in Fig. 3. In the transmitter program, the transmitted I/Q data samples are up-sampled by a factor T. Then the I/Q samples are filtered by symmetric ht[n]s in I channel and Q channel, respectively. Next, these samples are sent to the bladeRF SDR platform. In bladeRF, these I/Q samples are first converted to analog forms by digital-to-analog converters (DACs), up-converted to 900-MHz band, and then are sent out through the Tx antenna. The distance between the Tx antenna and the Rx antenna is 1.5 m. At the receiver part, the received RF signal is down-converted to baseband I/Q signals. Next, the I/Q signals are sampled by analog-to-digital converters (ADCs) to I/Q samples in the bladeRF platform. These samples are sent back to the computer and are processed by the receiver program. In the receiver program, these I/Q samples are filtered by the same symmetric ht[n]s and next are down-sampled to obtain the I/Q data samples. A packet of I/Q data samples are next mapped to form a constellation and are detected as symbols. Finally, we compare the detected symbols with the transmitted symbols and accumulate the number of error symbols. After sufficient error symbols are accumulated, we can calculate the SER.

In the experiment, each packet contains 2048 I/Q symbols including 48 preamble symbols. These preamble symbols are known a priori for the receiver that the receiver can use them to make the demodulated constellation possess a correct orientation. Fig. 4 shows the picture of an example received 16-QAM constellation.

III. EXPERIMENT RESULTS AND DISCUSSIONS

As mentioned in Section I, many modern electronic communication systems, e.g. the SDR platform in this experiment, employ high speed ADC to convert the received signal to digital form. Then the synchronization work is done in the digital domain. That is, no perfect clock recovery circuit is used in the system. Under such circumstance and $T = 4$, we observe burst errors happen from time to time at the receiver. Hence, it is difficult to accurately measure the SER. In this experiment, the procedure is as follows. First, we program the transmitter's variable gain amplifier and calculate the estimated SNR. Next we count the number of incorrect symbols. After the first burst of errors is observed, we stop the receiver program and record the number of received symbols and the number of incorrect symbols. Then the SER after the first burst of errors is obtained.

Fig. 5 shows the experiment results. Since the occurrence of the burst errors and the length of an error burst are unpredictable, the tendency of the SER after the first burst of errors is not monotonic. On the other hand, the SER after the first burst of errors resulted from using the proposed SR filters is mostly better than that resulted from using the SR filters designed by the method of [11]. This situation is unlike the

conventional SER study, in which the SER curve is monotonic and one SER curve seldom crosses the other SER curve. Our explanation of the above unusual cases is that the burst errors are completely unpredictable.

Fig. 3 Picture of the experiment

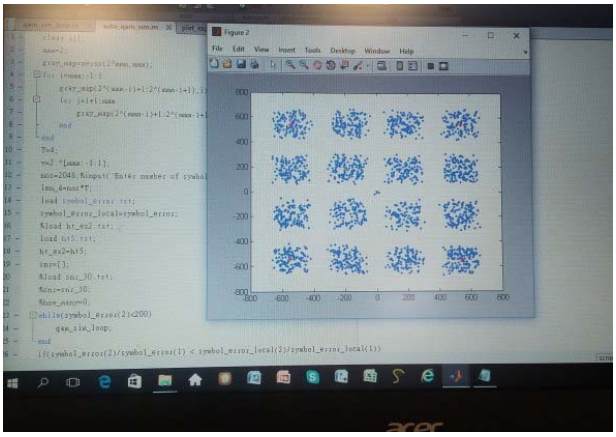

Fig. 4 Picture of a demodulated constellation in the experiment

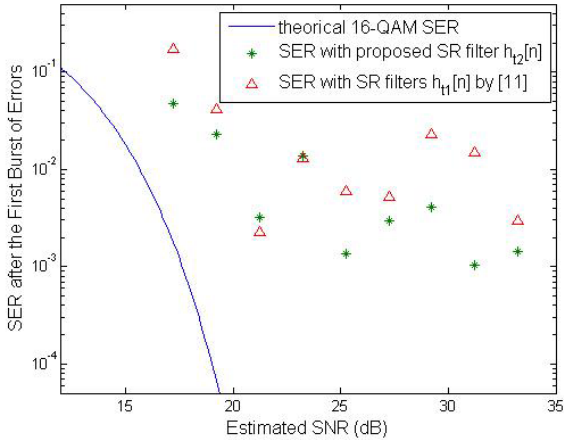

Fig. 5 SER after the first burst of errors in the 16-QAM experiment with $T = 4$

To investigate why we encountered burst errors in this experiment, we increase the oversampling ratio T to 8 in the subsequent experiments. We redesign two 37-tap SR filters, $h_{t3}[n]$ and $h_{t4}[n]$, by the method of [11] and by the method of [12], respectively. We then experiment on a 64-QAM system. Table III shows the designed SR filters' coefficients and Fig. 6 shows a 64-QAM constellation example at the receiver. The SER plot is shown in Fig. 7. We observe that when the oversampling ratio is sufficiently large, the phenomenon of error burst seldom happens and the SER plot possesses a regular monotonic behavior. Therefore, we can say that when the value of the oversampling ratio is small, it is not easy to realize a sufficiently good clock recovery subsystem in the digital domain and the overall system is prone to having burst of errors. Hence, although using a high-speed ADC in a modern communication system helps to alleviate the analog design effort, we note that using a sufficiently large oversampling ratio is required. On the other hand, we also note that the SER of the 64-QAM experiment employing the SR filter designed by minimizing the roughness value [12] outperforms that employing the SR filter designed by minimizing the PAR value [11].

TABLE III
SYMMETRIC SR FILTER COEFFICIENTS OF $H_{t3}[N]$ DESIGNED BY THE METHOD OF [11] AND $H_{t4}[N]$ BY THE METHOD OF [12]

$h_{t3}[n]$: Length = 37, $h_{t3}[n] = h_{t3}[36 - n]$, $n = 19, 20, \ldots, 36$	
$h_{t3}[0] = 2.6124710 \times 10^{-3}$	$h_{t3}[10] = -1.2855040 \times 10^{-2}$
$h_{t3}[1] = 4.3436944 \times 10^{-3}$	$h_{t3}[11] = 3.7691437 \times 10^{-4}$
$h_{t3}[2] = 5.0235414 \times 10^{-3}$	$h_{t3}[12] = 2.0287260 \times 10^{-2}$
$h_{t3}[3] = 3.9685220 \times 10^{-3}$	$h_{t3}[13] = 4.5284600 \times 10^{-2}$
$h_{t3}[4] = 8.0976066 \times 10^{-4}$	$h_{t3}[14] = 7.2745056 \times 10^{-2}$
$h_{t3}[5] = -4.2718283 \times 10^{-3}$	$h_{t3}[15] = 9.9384907 \times 10^{-2}$
$h_{t3}[6] = -1.0510008 \times 10^{-2}$	$h_{t3}[16] = 1.2166906 \times 10^{-1}$
$h_{t3}[7] = -1.6380993 \times 10^{-2}$	$h_{t3}[17] = 1.3647760 \times 10^{-1}$
$h_{t3}[8] = -1.9991033 \times 10^{-2}$	$h_{t3}[18] = 1.4166768 \times 10^{-1}$
$h_{t3}[9] = -1.9358533 \times 10^{-2}$	
$h_{t4}[n]$: Length = 37, $h_{t4}[n] = h_{t4}[36 - n]$, $n = 19, 20, \ldots, 36$	
$h_{t4}[0] = 2.5643705 \times 10^{-3}$	$h_{t4}[10] = -1.2971103 \times 10^{-2}$
$h_{t4}[1] = 5.2844809 \times 10^{-3}$	$h_{t4}[11] = 2.3263774 \times 10^{-3}$
$h_{t4}[2] = 6.6863488 \times 10^{-3}$	$h_{t4}[12] = 2.3528516 \times 10^{-2}$
$h_{t4}[3] = 5.6687536 \times 10^{-3}$	$h_{t4}[13] = 4.8691514 \times 10^{-2}$
$h_{t4}[4] = 1.7355209 \times 10^{-3}$	$h_{t4}[14] = 7.5145481 \times 10^{-2}$
$h_{t4}[5] = -4.8097854 \times 10^{-3}$	$h_{t4}[15] = 1.0004593 \times 10^{-1}$
$h_{t4}[6] = -1.2749066 \times 10^{-2}$	$h_{t4}[16] = 1.2048702 \times 10^{-1}$
$h_{t4}[7] = -1.9699380 \times 10^{-2}$	$h_{t4}[17] = 1.3391898 \times 10^{-1}$
$h_{t4}[8] = -2.3269750 \times 10^{-2}$	$h_{t4}[18] = 1.3860209 \times 10^{-1}$
$h_{t4}[9] = -2.1438097 \times 10^{-2}$	

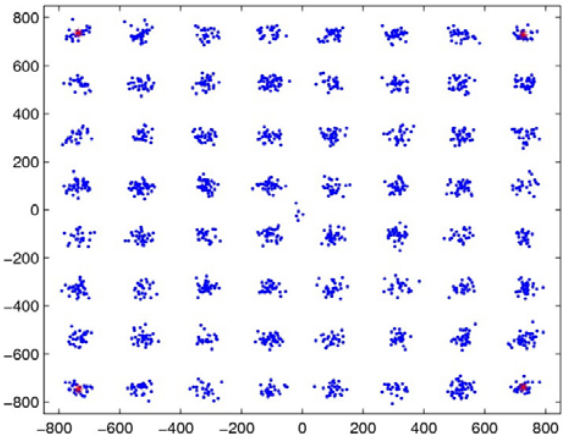

Fig. 6 A receiver 64-QAM constellation example with $T = 8$

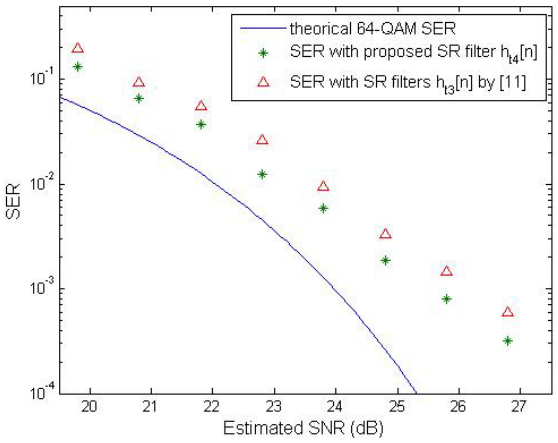

Fig. 7 SER of the 64-QAM experiment with $T = 8$

IV. Conclusion

In this paper, we experiment with error performances of QAM systems employing SR filters designed by minimizing the roughness value and by minimizing the PAR value on the bladeRF SDR platform. Two observations are obtained. First, if the oversampling ratio is not high enough, the QAM system will be prone to have error burst because the quality of the clock recovery subsystem is poor in this case. Hence, the quality of communication will be poor, too. Second, when the oversampling ratio is high enough, the QAM system employing SR filters designed by minimizing the roughness value performs better than the QAM system employing SR filters designed by minimizing the PAR value.

Acknowledgment

The authors would like to thank the Nuand LLC for providing many design examples that help us with completing the experiments in this project.

References

[1] J. O. Coleman and D. W. Lytle, "Linear-programming techniques for the control of intersymbol interference with hybrid FIR/analog pulse shaping," in *Proc. IEEE Int. Conf. Commun.*, Chicago, IL, June 1992, pp. 793–798.

[2] J. O. Coleman, "Linear-programming design of data-communication pulses tolerant of timing jitter or multipath," in *Proc. Fifth Int. Conf. Wireless Commun.*, Calgary, Canada, July 1993, pp. 341–352.

[3] C.-Y. Yao and A. N. Willson, Jr., "The design of asymmetrical square-root pulse-shaping filters with wide eye-openings," in *Proc. 2008 IEEE Int. Symp. Circuits Syst*., May 2008, pp. 2665–2668.

[4] B. Farhang-Boroujeny and G. Mathew, "Nyquist filters with robust performance against timing jitter," *IEEE Trans. Signal Processing*, vol. 46, pp. 3427–3431, Dec. 1998.

[5] T. N. Davidson, Z.-Q. Luo, and K. M. Wong, "Design of orthogonal pulse shapes for communications via semidefinite programming," *IEEE Trans. Signal Processing*, vol. 48, pp. 1433–1445, May 2000.

[6] T. N. Davidson, "Efficient design of waveforms for robust pulse amplitude modulation," *IEEE Trans. Signal Processing*, vol. 49, pp. 3098–3111, Dec. 2001.

[7] C.-Y. Yao, "The design of hybrid asymmetric-FIR/analog pulse-shaping filters against receiver timing jitter," *IEEE Trans. Commun.*, vol. 60, pp. 1199-1203, May 2012.

[8] P. Siohan and F. M. de Saint-Martin, "New designs of linear-phase transmitter and receiver filters for digital transmission systems," *IEEE Trans. Circuits. Syst. II*, vol. 46, pp. 428–433, Apr. 1999.

[9] C.-Y. Yao, "The design of square-root-raised-cosine FI R filters by an iterative technique," *IEICE Trans. Fundamentals*, vol. E90-A, pp. 241–248, Jan. 2007.

[10] C.-Y. Yao and A. N. Willson, Jr., "The design of symmetric square-root pulse-shaping filters for transmitters and receivers," in *Proc. 2007 IEEE Int. Symp. Circuits Syst*., May 2007, pp. 2056–2059.

[11] B. Farhang-Boroujeny, "A square-root Nyquist (M) filter design for digital communication systems," *IEEE Trans. Signal Processing*, vol. 56, pp. 2127–2132, May 2008.

[12] C.-Y. Yao and A. N. Willson, Jr., "The design of hybrid symmetric-FIR/analog pulse-shaping filters," *IEEE Trans. Signal Processing*, vol. 60, pp. 2060-2065, Apr. 2012.